LOW-β SC RF CAVITY INVESTIGATIONS

E. Zaplatin, W. Braeutigam, R. Stassen, FZJ, Juelich, Germany

Abstract

At present, many accelerators favour the use of SC cavities as accelerating RF structures. For some of them, like long pulse Spallation Source or Transmutation Facility SC structures might be the only option.

For the high energy parts of such accelerators the well-developed multi-cell elliptic cavities are the most optimal. For the low energy part the elliptic structures cannot be used because of their mechanic characteristics. There is a scope of different already proven low-β SC cavities. Here we investigate so-called quarter-wave coaxial cavities (160 MHz, β=0.11 and 320MHz, β=0.22) and based on spoke cavity geometry multi-cell H-cavities (700 and 350 MHz, β=0.2-0.5). All cavities optimised to reach the maximal possible accelerating electric field. The results of electrodynamics and structural analysis are presented. Some conclusions on cavity mechanical stability are made. The simulations also have been done for various vacuum and coupling port positions. Different cavity tuning schemes are under investigation and compared results are presented.

The comparison of numerical simulations with first experimental results of 700 MHz, β=0.2 10-gap H-cavity copper model measurements are shown.

1 QUARTER- AND HALF-WAVE CAVITIES

Quarter-Wave RF Resonator (QWR) is a coaxial transmission line shortened by the terminating capacitance. The range of such structure application is for rather low β<0.2 and fundamental frequency under 300 MHz. The resonant frequency is defined by the line length, inner-outer radius ratio and capacitance. An accelerating field magnitude is limited by peak magnetic field that is defined mainly by the radius of the inner electrode. This favours the use of the cone QWR (Fig.1). The disadvantage of the cone cavity is larger longitudinal extension, which still can be compensated by the accelerating field increase (Table 1).

Figure 1: Cone Quarter-Wave Resonator.

The weak point of any QWR is its non-symmetry, which results in transversal components (especially magnetic) of RF field on the beam path. This can be eliminated by the half-wave coaxial cavity use.

Table 1: Quarter- and Half –Wave Cavity Parameters

	Cyl. QWR	**Cone QWR**	**Cone HWR**
Freq. (MHz)	160	160	160
β=v/c	0.11	0.11	0.11
Rcav (cm)	9	18	18
Rin.elec. cm)	3	3	3
Lcav. (cm)	51.5	48.2	112
R apper. (cm)	1	1	1
Epk/Eacc	5.09	5.04	4.85
Bpk/Eacc (mT/MV/m)	11.41	6.72	7.25

2 SPOKE AND H-CAVITIES

2.1 Cavity Optimisation

The spoke cavity (Fig.2)[1] by definition is a coaxial half-wave length cavity with an outer conductor turned on ninety degrees so that its axes is directed along the beam path. An equivalent capacitance of such cavity is defined by the distance between conductors in the centre of the cavity along this axe. The range of application of this cavity is from 100 to 800 MHz of fundamental frequency and β=0.1-0.6. The limitations of application are defined mainly by the resonance capacitance grow for low β values which in its turn reduces cavity diameter.

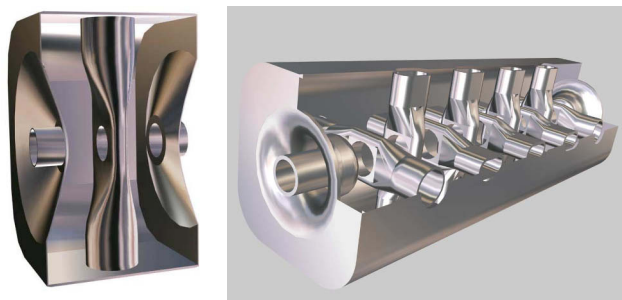

Figure 2: Spoke & 10-Gap H-Cavities (700 MHz, β=0.2)

To simplify the cryostat and control system design and to reduce the total accelerator length the multy-gap structure based on spoke cavity design is under consideration. Such structure could represent the same cylindrical or modified shape outer conductor as the cavity tank loaded with several electrodes (Fig.2). But as soon as one adds at least another spoke in such structure it turns from the coaxial spoke cavity into H-type cavity, which is defined by the electromagnetic field distribution. The detailed results of multy-gap H-cavity optimisation are published elsewhere[2]. Single gap simulations have provided the spoke shape optimisation with symmetry planes as the boundary conditions. This defines π-mode like accelerating field distribution along multy-gap structure. During simulations we supposed the spoke

manufacture by deforming the bulk Nb pipe, which means the spoke circumference in any cross section the same. Fig.3 presents the plots that used as the measures for optimisations. Co-dimensions of the spoke, accelerating gap and cavity tank size define the peak electric field. The optimum corresponds to the electric field homogeneous distribution on the spoke surface.

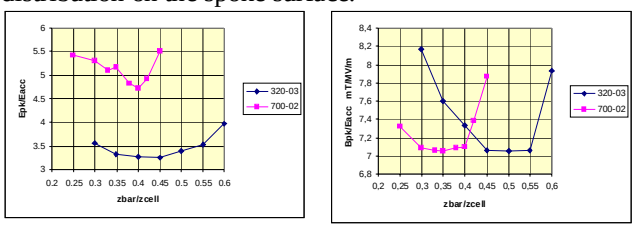

Figure 3: Spoke Geometry Optimisation

In the single spoke (two gaps) cavity the most optimal spoke shape in the base region is the cylindrical cross-section. It is resulted from magnetic field distribution that surrounds an electrode. But the main limitation on B_{pk} comes from the interaction with the cavity walls. To increase the space available for RF magnetic field we propose to make cavity tank square rather cylindrical (Fig.2). Another modification is related to the spoke geometry. In the H-type cavity the main magnetic flux distributes along the cavity length. That's why we suggest making spoke plane not only in the centre but also in the base parts. This brings not only again more space for h-field but mainly makes the distribution of the current on the spoke more homogeneous (Fig.4). Such modifications result in 25% reduction of B_{pk}/E_{acc} ratio.

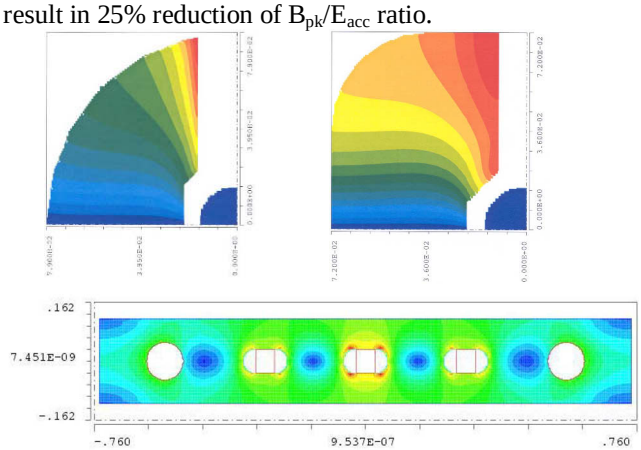

Figure 4: H-Cavity Geometry Optimisation

Table 2: SC H-Cavity Parameters

Freq. (MHz)	700	700	700	320	320
β=v/c	0.2	0.4	0.5	0.22	0.3
Rcav (cm)	7.15	9.1	9.2	15.2	16.5
Rapp. (cm)	1.5	1.5	1.5	1.5	1.5
E_{pk}/E_{acc}	5.10	3.88	3.79	4.6	3.3
B_{pk}/E_{acc} (mT/MV/m)	7.06	8.03	9.76	6.4	7.05

The results of the numerical simulations of such type structures are summarised in Table 2. For the cavities with higher β's we used scaled geometry configurations which resulted not in optimal cavity parameters.

There is a possibility to use completely connected spoke bases getting the structure similar to a 4-vane RFQ cavity (Fig.5). To our mind it complicates much the cavity manufacture. The RF parameters and electric field distribution along cavity are similar to the previous structure. The radius of vane ends defines the limitation on magnetic field. This is a reason why the last spokes should be made with round bases.

Figure 5: 10-Gap SCH with Bars (320 MHz, β=0.3)

To create an even distribution of an electric field along the beam path we use additional volumes in the end parts of the cavity and decreased last accelerating gaps. This adds more space for magnetic field in this region, increases capacitance of gaps and as a result modifies e-field profile (Fig.6).

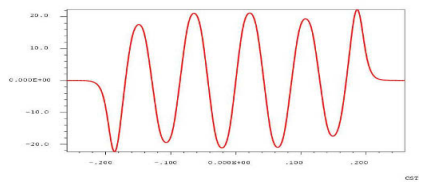

Figure 6: Accelerating Field along Beam Path in 10-Gap H-Cavity

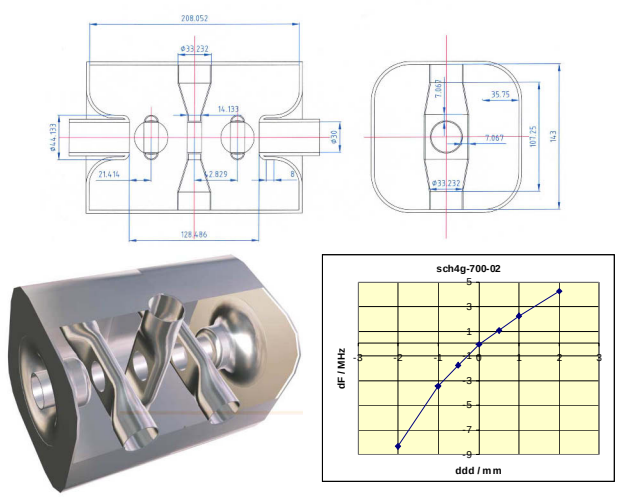

Figure 7: 4-gap H-cavity Geometry & Tuning Curve

As a first step of an experimental SC H-cavity investigation we plan to build 4-gap 700 MHz, β=0.2

cavity (Fig.7). The main structure dimensions are kept like for 10-gap 700 MHz, β=0.2 cavity. The change in geometry has been made only for the end regions to have homogeneous electric field distribution along cavity axe.

2.2 Cavity Tune and Coupling

For the cavity fine frequency tune the back walls of the structure can be used. The conjunction of these walls to the end electrodes is made round to give flexibility for their mechanic deformation. A frequency change is made by push-pulling this back planes. Electrically it means the last gap capacitance change and the possible frequency range change is defined by the last gap size. Here (Fig.7) the tuning is made only on one side of the cavity. The field profile changes within +30/-20% by +/-2 mm gap change. As an alternative option we consider an inductive tuner[3] which is installed in the end region at the maximum magnetic field (Fig.8). The possible frequency shift is up to 2.5 MHz.

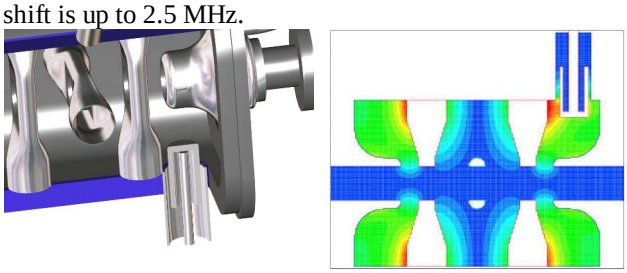

Figure 8: 4-Gap SCH-Cavity with Inductive Plunger (geometry & magnetic field distribution)

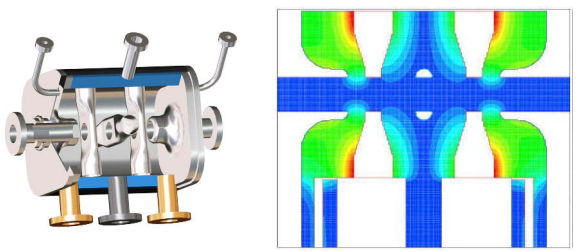

Figure 9: 4-Gap SCH-Cavity with Coupling Ports (geometry & magnetic field distribution)

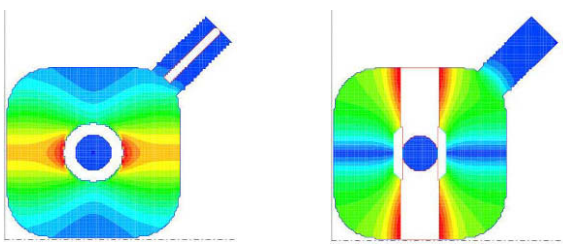

Figure 10: 4-Gap SCH-Cavity with Coupling Ports turned on 45° (magnetic field distribution)

Two possible places for vacuum and coupling ports are considered. First (Fig.9) is the plane side cavity wall, which has an advantage that the vacuum port is situated in the centre of the cavity with a minimal RF electromagnetic field. At the same time the power coupling and probe ports are close to the maximal RF magnetic field which makes the coupling easy. Another positive point is a plane conjunction place for ports with walls. The second option (Fig.10) – connection at the round cavity corners. The reason of this choice is to increase the efficiency of use the port holes to get the cavity wall treatment fluid out.

2.3 10-Gap H-Cavity Copper Model

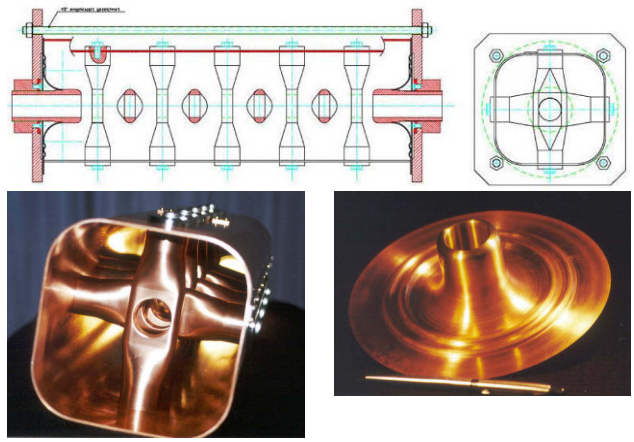

Figure 11: 10-gap H-cavity Copper Model

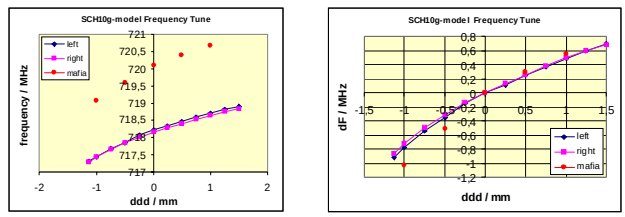

Figure 12: Resonance frequency & frequency shift vs. last accelerating gap change

The simulations for the field profile and cavity tuning have been made with MAFIA codes for ¼ part of geometry with around 2.5M mesh points.

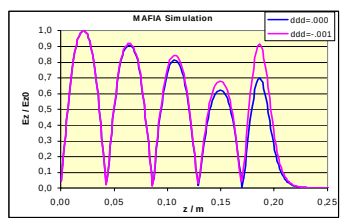

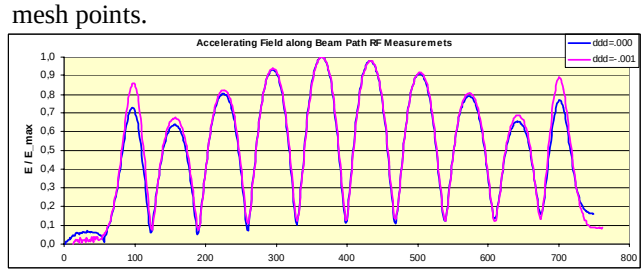

Figure 13: Electric Field Distribution along Beam Path (simulation & measurements)

For 3D numerical simulation verification and cavity tuning investigation 10-gap H-cavity copper model (700 MHz, β=0.2) has been built (Fig.11). The cavity and end

plates are made from the 3 mm and 1 mm copper sheet respectively. The spokes have been machined from the bulk copper. For the cavity tune the deformation of the end plates is used. The results of the numerical simulations and first model measurements are shown on Figs.12-13.

3 STRUCTURAL ANALYSIS

The structural analysis of SC H-cavity has been made to find the model predictions for peak stresses, deflections and flange reaction forces under vacuum loads and room temperature, and also for forces required to produce a specify tuning deflection. The important part of simulations is devoted to the determination of resonant structural frequencies.

The whole H-cavity is supposed to be produced out of niobium sheets. The following parameters of niobium are used:

- Young's modulus E=105000 N/mm^2,
- Density ρ=8.57 g/cm^3,
- Poisson number ν=0.38.

The Young's modulus of niobium is in the wide temperature range invariable, also in the range of the cryo-temperatures. We use yield strength 500 MPa as a reference measure[4] in our calculations.

The simulations have been made with ANSYS codes.

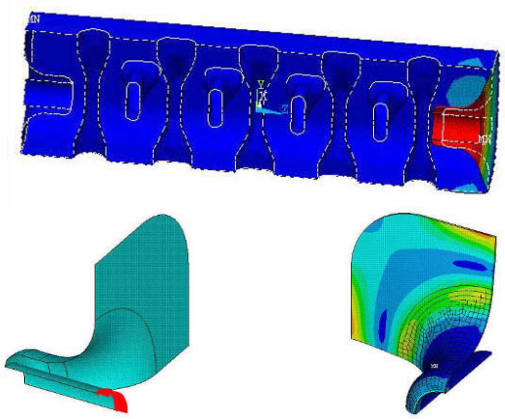

Figure 14: 10-gap H-cavity Tuning Simulation (deformations, force application, von Mises stress)

3.1 Tuning and Vacuum Pressure

To allow the cavity tuning by the end plate deformation it should be flexible enough and at the same time rather rigid to keep an extra pressure from the helium volume and cool-down stress. The end electrode shift for tuning should be in the range of +/-2 mm (which is defined by cavity cross section size) that makes about +/-0.5 MHz frequency shift for 320 MHz, β=0.3 10-gap cavity. For 700 MHz, β=0.2 cavities it is much better (Figs.7,12). The required forces for such deformations are 65.6 kN (10-gaps, 700 MHz, β=0.2) and 12.96 kN (10-gaps, 320 MHz, β=0.3). No any other serious deformations detected in the cavity shape (Fig.14).

In the analysis of the cavities under vacuum loading conditions all structure surfaces are under 1 atm extra atmospheric pressure including the surfaces of spokes as they are supposed to be filled with a liquid helium.

Table 3: Deformations Caused by Extra Pressure in 10-Gap H-cavities

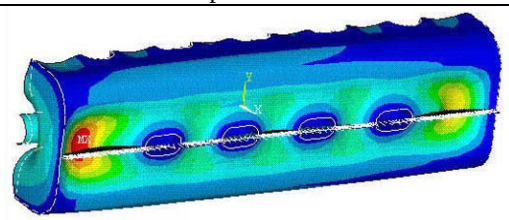

SCH10-700-02	SCH10-320-03
End Plate: Wall thickness 1 mm Max deformation 0.5e-6 m Max stress von Mises 0.35 MPa	End Plate: Wall thickness 1 mm Max deformation 0.8e-4 m Max stress von Mises 10.3 MPa
Walls (No Stiffening Ribs): Wall thickness 2 mm Max deformation 1.9e-5 m Max stress von Mises 9.9 MPa	Walls (No Stiffening Ribs): Wall thickness 3 mm Max deformation 1.6e-3 m Max stress von Mises 193 MPa
Walls (Stiffening Ribs): Wall thickness 2 mm Ribs 1cm high, 2 mm thick Max deformation 8.3e-6 m Max stress von Mises 9.3 MPa	Walls (Stiffening Ribs): Wall thickness 2 mm Ribs 2cm high, 5 mm thick Max deformation 0.2e-3 m Max stress von Mises 120 MPa

For comparison we calculated the cavities with longitudinal ribs welded along two structure sides with maximal predicted deformations (Table 4). The 700 MHz, β=0.2 cavity because of its small dimensions is able to work without stiffening. The 320 MHz, β=0.3 cavity needs stiffening but on the other hand the single rib per cavity side going direct through the spoke-wall contact places may not be practical in terms of cavity manufacture. In this case we simulated two ribs per cavity side. The results are about in the same range. The highest stresses are always at spoke-wall joints.

3.2 Cool-Down

The cavity is supposed to be assembled at room temperature and then cooled to 2-4 K in a fluid helium bath. As the cool gas and liquid enter through the vent pipe at the top of the helium vessel, localized cooling occurs for components directly in line with the coolant flow. The localised cooling results in thermal and stress gradients. As a start up we investigate cavity geometry displacements and loads under temperature gradient and steady-state cool-down conditions. More accurate and full calculations have to be made during cavity-helium vessel assembly design. Here we limit ourselves by the case of cavity degree of freedom with both beam pipes and tuning plates at their external circumference are fixed. In the real

design some addition suspensions like vacuum and coupling ports will make the structure even more rigid.

To simulate the transient cooling of the cavity the bottom side was cooled to 2 K, while the rest remained at 293 K. Fig.15 shows deformed geometry without additional pressure applied. The transient case tends to shrink the cavity bottom causing the maximal stress in the spoke-wall joints. The stresses in the cavity well below the design allowable. In steady-state case the whole cavity is under 2-4 K operating temperature.

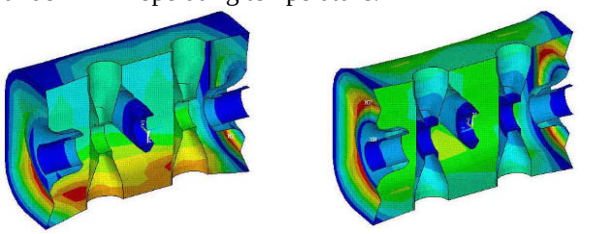

Transient Cooling:
Max Displacement 0.273 (mm)
Max Stress von Mises 431 (Pa)

Steady-State Cooling:
Max Displacement 0.413 (mm)
Max Stress von Mises 633 (Pa)

Figure 15: Cool-Down Simulations of 4-gap H-cavity (700 MHz, β=0.2)

As a final simulation we investigated combined case with cool-down, vacuum pressure and tuning altogether. The results are summarised in Table 4.

Table 4: Cavity Structural Analysis with Cool-Down, Vacuum Pressure and Tuning (SCH4-700-02).

Tuning	-2 mm	+2 mm
Tuning Pressure	16.37 kN	55.33 kN
Max Displacement	-2.6 mm	+2 mm
Von Mises Stress	870 MPa	679 MPa

3.3 Modal Analysis

Table 5. Modal Analysis Results of Spoke Cavity

Spoke Cavity 700 - 0.2	**Spoke Cavity 320 - 0.3**	**Spoke Cavity 320 - 0.3**
Frequency / Hz	*Frequency / Hz*	*Frequency / Hz*
walls 2/1	walls 2/1	walls 3/3
275.179	50.1	94.853
492.504	57.452	75.506
589.763	74.267	150.375
698.115	74.606	152.544
698.122	86.655	144.097
815.524	92.018	255.193
877.013	162.638	176.949
1053	164.155	266.892

The main purpose of these simulations is to find weak points of the cavity in terms of dynamic behaviour to make subsequently design of a most optimal rigid outer containment. The boundary conditions (constrains) for all our models are the both beam pipe ends completely blocked against displacements in any direction (by tuner or continuos beam pipe). Additionally, in 10-gap cavity calculations we fixed also the outer cavity tank at one side. In a real cavity design together with cryostat most probably both cavity ends will be fixed. In the future, more accurate and detailed calculations with a real cryostat design should be provided. The following simulations show the first results, which give a representation about mechanical stability of such cavities (Tables 5-7). Detailed results one can find elsewhere[5].

Table 6. Modal Analysis Results of 4-Gap H-Cavity

SCH4-700-0.2	
Frequency / Hz	*Frequency / Hz*
walls 2/1	walls 3/3
125.435	327.659
235.935	434.449
238.875	449.598
251.018	333.436
283.487	550.072
285.227	568.97
543.119	732.491

Table 7. Modal Analysis Results of Spoke Cavity

SCH10-700-0.2	**SCH10-320-0.3**	**SCH10-320-0.3**	**SCH10-320-0.3**
	both cavity ends fixed		
Freq / Hz	*Freq / Hz*	*Freq / Hz*	*Freq / Hz*
walls 2/1	walls 3/1	walls 3/1 + rib/side	walls 3/1 + 2 ribs/side
284.287	86.512	113.552	94.078
284.418	114.539	196.821	153.138
387.09	145.107	287.855	225.853
392.318	165.344	306.677	275.263
469.385	167.795	306.677	286.433
477.744	240.284	316.893	303.925
542.391	256.78	322.188	339.284

4 REFERENCES

[1] J.R. Delayen et al., "Design and Test of a Superconducting Structure for High-Velocity Ions", LINAC'92, Ottawa, 1992.

[2] E.N. Zaplatin, "A Spoke RF Cavity Simulation with MAFIA", RFSC'99, Santa Fe, 1999.

[3] Yu. Senichev, T. Korsbjerg, S.P. Moeller, E. Zaplatin, "Solving the Problem of Heating of RF Contacts in Cavity Tuners", Pac'97, Vancouver, 1997.

[4] R.P. Walsh et al., "Low Temperature Tensile and Fracture Toughness Properties of SCRF Cavity Structural Material ", SCRF'99, Santa Fe, 1999.

[5] E.N. Zaplatin, "Electrodynamics and Mechanical Features of H-Type Superconducting Structures for Low Energy Part of ESS Linac", ESS 01-116-L, Juelich, 2001.